THERMAL DEGRADATION AND KINETIC STUDY OF VINYL MONOMER GRAFTED SILK FIBROIN

Archana M. Das, Abdul A. Ali and Manash P. Hazarika

***Abstract*— Modification of biodegradable protein fibre - *Anthearea assama* silk (SH) has been carried out by graft copolymerization using methylmethacrylate (MMA) with cerric ammonium sulphate. The thermal properties have been characterized by thermogravimetric analysis (TGA), differential thermogravimetry, differential thermal analysis and differential scanning calorimetry techniques. The kinetic parameters have been studied using Broido method with FORTRAN 77 computer programming and calculated the activation energy. And also the influence of the reactants on the resulted product has been examined. In comparison with the conventional SH, the resulted methylmethacrylate grafted *Anthearea assama* silk (SHMMA) have improved thermostability properties. The strategy described here a potential alternative to the new technique for thermostable grafted products. The structural changes of SHMMA, changes of the crystalline and amorphous ratio after grafted with MMA-Ce^{IV} initiator had been studied in relation to the weight gain and X-ray diffraction curves.**

***Index Terms*— Activation energy, *Antheraea assama*, Broido method, Graft copolymerization, Kinetic parameters, Methylmethacrylate, Vinyl monomer.**

I. INTRODUCTION

Modification of natural or synthetic fibroin with the aim, of imparting specific properties to the products has given a great thrust to macromolecular science. Targeted and desirable properties can be imparted to the fibroin through grafting, in order to meet the requirement of specialized applications. It is a very usefull and convenient technique for altering the properties of numerous polymer back-bones and make with a number of new advantageous properties [1]. Recent interest lies on the application of biomaterials- silk fibroin (SH) due to its unique mechanical properties as well as the biocompatibility and biodegradability [2]. Silk fibers exhibit high wear resistance and physicomechanical properties making their wearing comfortable, good capability of silk fibers for moisture absorption, air permeability, and low electrifiableness [3]. This silk fibroin is a well described natural fiber produced by the silkworm, *Antheraea assama* Westwood (Lepidoptera:Saturniidae), a multivoltine, sericogenic insect, popularly known as muga silk and has natural golden yellow hue. It is one of the most important and commercially valuable silk varieties native to North Eastern India [4], which has been used traditionally in the form of thread in textiles for thousands of years. This Silk fiber having two primary components, one is fibroin and another is sericin. Fibroin is the major component, which accounts for about 70% of novel silk fibers, and sericin is another kind of silk protein, which accounts for about 30% of silk fibers [5]. Recently, SF fiber from silkcocoons (e.g., *Bombyx mori*) has been explored to exploit the properties of this protein as biomaterial [6-8], cosmetics creams, lotions, makeup, powder, bath preparations and pharmaceuticals due to its excellent characters as textile fiber. Moreover, the natural silk fiber is one of the strongest and toughest materials mainly because of the dominance of well orientated β-sheet structures of protein chains [9-10].

Moreover, recent work demonstrates the ability of silk films to serve as a platform for tissue engineering, transistors [11] and various classes of photonic devices [12-13]. The interpretation of polymerization kinetics demands knowledge of reliable kinetic parameters and provide the basis for more accurate design of polymerization reactions and better insight into the behaviour of existing reactions [14]. The thermoanalysis methods help us to find the temperature at which enough radicals are formed to initiate the reaction efficiently. Although the literature contains an abundance of initiator decomposition rates in various solvents [15], the in situ rate data for polymerization systems are scarce. Differential thermoanalysis methods, such as thermogravimetry (TG), differential thermogravimetric analysis, differential thermal analysis and differential scanning calorimetry (DSC), etc. have been used for kinetic studies of reacting systems [16]. The results of these experiments are usually represented by a curve, the features of which (peaks, discontinuities, changes in slop, etc.) can be related to the thermal events in the samples.

In this manuscript we have tried to discuss about the thermal degradation behavior by thermogravimetric analysis (TGA), differential thermogravimetry (DTG), differential thermal analysis (DTA) and differential scanning calorimetry (DSC), kinetic parameters, crystallinity by X-ray diffraction and the structure determination of the SHMMA have been studied.

II. EXPERIMENTAL SECTION

A. Materials.

Muga reeled silk, produced by following standard degumming and reeling method [17] was collected from a private farm near Jorhat, Assam, India. As the silk fibroin was processed ready for weaving, no further purification was rendered. Methylmethacrylate (MMA) was first washed with 5% NaOH solution, and then dried with anhydrous sodium sulphate and distilled under nitrogen in reduced pressure [18]. Ceric ammonium sulphate (E-Merck), silica gel (CDH),

Manuscript received Feb. 12, 2014.
Archana M. Das, Natural Products Chemistry Division CSIR-North East Institute of Science & Technology Jorhat – 785 006, Assam, India.

H_2SO_4 (AR, BDH) and acetone (CDH), distilled water were used for this study.

B. Graft copolymerization procedure

All the polymerization reactions were carried out in air as the use of nitrogen atmosphere during the time of reaction was found to have no significant contribution on conversions to the products [19]. The reaction was set up in a three necked 300 ml round bottom flask fitted with stirrer in a temperature controlled water bath. 1 g dry silk fibre/fabric of 10 mm length was swollen with water for 15 min and it was transferred to the reaction flask containing solutions of ceric ammonium sulphate and H_2SO_4 of different concentrations. The required amount of monomer (MMA), was added to the reaction system at the required temperature. The reaction time was varied from 1h-5 h and temperature of reaction from 35 ^{0} -65 ^{0}C at material to liquor ratio 1:150 and intermittently stirred the reaction system. After the desired reaction time, products were taken out and were then subjected to repeated extraction with boiling water and acetone to remove homopolymer and its oligomers adhering to the silks. Finally, the products were dried to constant weight and kept in desiccators over P_2O_5. For characterization, the silk samples were cut into fine pieces by scissor and pass through 350 mesh to get power form.

2.3 Thermal Analysis of Copolymers

Thermo-gravimetric analysis (TGA), differential thermogravimetric (DTG) and differential thermal analysis (DTA) were carried out using a Shimadzu (Model 30) thermal analyzer. The masses of the samples were in the range 3.95-5.78 mg. □-alumina was used as a reference material and the temperature ranged from 30- 800 ^{0}C at heating rates of 10^0, 20^0 and 30^{0}C min^{-1} in a static air atmosphere. DSC was obtained from a Perkin-Elmer DSC-7 with kinetic software. It consists of a compact central unit and family of cells for DSC thermogravimetry and thermochemical analysis. The heart of the system, the TA processor, functions as a combination of control unit, computer power unit and interface to be used through the key board and display. The DSC 20 standard cell is used for heat flow measurement in the temperature range ambient to 800 ^{0}C.

a) 2.3.1 Theoretical Approach for Kinetic Studies

The kinetics of polymer degradation is usually represented by the basic kinetic equation (1) [20].

$$d\alpha/dt = k(T)f(\alpha) \qquad (1)$$

Where, α represent the conversion (extent of reaction; a = 0-1), t is the time, k(T) is the rate constant , and f(□) is the reaction model, which describes the dependence of the reaction rate on the extent of reaction. Temperature dependence of k(T) could be represented by the Arrhenius equation (2)

$$d\alpha/dt = Ae^{-Ea/RT} f(\alpha) \qquad (2)$$

where *Ea* is the activation energy of the process. A is the pre-exponential factor, R is the universal gas constant, and f(α) depends on the decomposition mechanism. The simplest and most frequently used model for f(α) is

$$f(\alpha) = (1-\alpha)^n$$
---------- (3)

where n is the order of reaction.

The rate of conversion, dα/dt, at constant temperature can be expressed by

$$d\alpha/dt = k = k(T)\, f(\alpha)$$
---------- (4)

and finally combining the equations 2, 3 and 4 gives the following relationship

$$d\alpha/dt = k = (1-\alpha)^n Ae^{-Ea/RT}$$
---------- (5)

and the equation (5) can be express for first order reaction by the following relationship

$$d\alpha/dt = k = Ae^{-Ea/RT}$$
---------- (6)

In short, the Arrhenius equation is an expression that shows the dependence of the rate constant *k* of chemical reactions on the temperature *T* and activation energy E_a, as shown above. In chemical kinetics a reaction rate constant quantifies the speed of a chemical reaction. In chemical kinetics, the frequency factor or A factor is the pre-exponential constant in the Arrhenius equation. The logarithm of the Arrhenius equation is represented by the following equation (7).

$$\ln(k) = -Ea/RT + \ln(A)$$

So, when a reaction obeys the Arrhenius equation, a plot of ln(*k*) versus T^{-1} gives a straight line, whose slope and intercept can be used to determine E_a and *A*. That is the activation energy defined to be (-*R*) times the slope of a plot of ln(*k*) vs. (1/*T*).

$$Ea = -R\,(\delta \ln k / \delta\,(1/T))$$
---------- (8)

Arrhenius equation gives the quantitative basis of the relationship between the activation energy and the rate at which a reaction proceeds.

2.3.2 Broido Method

The retrieval of kinetic parameters from weight loss versus temperature data could be carried out by using various methods [21-24]. In the present work, the well known Broido method [25] was used for retrieving kinetic parameters from dynamic thermogravimetry. The general correlation equation used in Broido method is:

$$\ln\left(\ln\frac{1}{y}\right) = -\frac{E_a}{R}\frac{1}{T} + \ln\left(\frac{R}{E_a}\frac{Z}{R_H}T_m^2\right)$$

Where, y is the fraction of the number of initial molecules not yet decomposed, R is the gas constant (KJ mol^{-1} K^{-1}), T is the temperature (K) and E_a is the activation energy (KJ mol^{-1}). Tm is the temperature of the maximum decomposition rate (K), R_H is the heating rate (K min^{-1}), and Z is the frequency factor (S^{-1}). Broido equation, as shown above, was used to determine the kinetic parameters for the first and second stage

of the thermal degradation of the polymer composites. A computer programme in FORTRAN 77 was used for the linear least square analysis with Gauss-Jordan sub-routine and applied to evaluate n, □ E, A and SED simultaneously. The procedure basically involved step wise change of the order of the reaction, n (over a range 0.6-1.6) to determine the SED in least square estimate of the parameters, □ E and A. The data were found to fit well for a first order reaction.

2.4 XRD of copolymers

X-ray diffraction data were collected using a computer controlled X-ray diffractometer (Type, JDX-11P3A, JEOL, Japan) with pulse-height analyzer and scintillation counter. Measuring conditions were: Mode, step; KV, 40; start angle 2 ^{0}; target, Cu; mA, 20; stop angle 60 ^{0}; measuring time 0.5 sec; step angle 0.05. The degree of crystallinity (Kc) was found out using the following equation [26].

$$Kc = \int_0^{\alpha} S^2 Ic(S)\, dS \Big/ \int_0^{\alpha} S^2 I(S)\, dS \quad \text{---------- (10)}$$

where S is the magnitude of reciprocal lattice vector and S is given by

$S = 2 \sin\theta / \lambda$

where θ is one half of the angle of deviation of the diffracted rays from the incident X-rays, λ is the X-ray wave length, I (S) is the intensity of coherent X-ray scatter from a specimen (both crystalline and amorphous), Ic (S) is the intensity of coherent X-ray scatter from the crystalline region.

2.5 Conditions Affecting Grafting

Grafting onto silk is a heterogeneous reaction and so physical structure and the state of aggregation of the silk fibre play an important role. The reaction involved whatever may be in grafting, chemical bonding is achieved and the synthetic polymer is associated in such a way that the components cannot be separated by the normal fractionation techniques. In the complex system of silk, monomer, initiator and acid, several reactions take place simultaneously as indicated above and the extent of grafting depends on the influence of chemical conditions, physical conditions and nature of substrate [27]. Chemical conditions involve (a) diffusion of monomer to the silk, (b) adsorption of the monomer on the silk, (c) initiation of the active sites on the silk side chain and backbone, (d) formation and propagation of graft on the silk, (e) termination of the active sites on the silk side chain and backbone, and (f) homopolymer formation. Physical conditions involve (a) swelling of silk and (b) accessibility of silk [28-30].

In regards to silk substrate, the fibres contain, both amorphous (disordered) and crystalline (ordered) regions, but there is no sharp boundary between the crystalline and disordered areas. Also, the fibres are though consisted of alternating regions of amorphous and crystalline structure, owing to this heterogeneous nature, graft copolymerization, particularly when performed in an aqueous medium, would be expected to be affected by the pore size of silk, the crystalline-amorphous ratio, the degree of orientation and the crystalline size [31].

III. Result and Discussion

3.1 Thermal analysis

The thermal behaviour of un-grafted and grafted products were studied from TG, DTG and DTA at heating rates 20 ^{0}C/min and 30 ^{0}C/min. TG, DTG and DTA curves for ungrafted and grafted products of different percentage of grafting for heating rate 20 ^{0}C/ min are shown in figure 1. The decomposition temperature ranges, the active decomposition temperatures and percent weight losses are given in Table 1(a) and Table 2(a) for grafted products of different percentages of grafting [32-33].

Thermal decomposition of fibres took place in three distinct stages referred to as initiation, propagation and carbonization. All the TG curves showed an initial small mass loss step around 150 ^{0}C, which could be attributed to the removal of absorbed water. In the second stage, a major weight loss was noticed at heating rate 20 ^{0}C/min for un-grafted and grafted products (49%, 59%, 71%). The decomposition of protein started at 150 ^{0}C for ungrafted, which increased for sample 49% grafted (175 ^{0}C), 59% grafted (185 ^{0}C) and 71% grafted (195 ^{0}C) depending on the increasing % of grafting, while in the third stage, decomposition of rest of the polymers started at 390 ^{0}C for ungrafted and increased for 49% grafted (440 ^{0}C), 59% grafted (455 ^{0}C) and 71% grafted (480 ^{0}C) (Table 1(a)) respectively. The weight loss (%) of the grafted fibre was found to be less than that of the un-grafted fibre as evident from Table 1(a) and 2(a), which showed the initial, maximum and final temperatures of active decomposition increased with increase in grafting (%) of the SHMMA in all the three heating rates. A similar trend was also observed at heating rate 30 ^{0}C/min. It was evident from Table 1(a) and 2(a), that in both the heating rates, the initial and maximum temperatures of decomposition increase with increased in grafting (%) for the SHMMA.

3.2 Kinetics Studies

To evaluate the kinetic parameters of SHMMA, we applied the Broido method using a computer programming FORTRAN 77 for linear least squares analysis with Gauss-Jordan subroutine. The degradation followed a first-order reaction, as assumed by Broido, the plots of ln(ln 1/y) versus (1/T) for the stages of the thermal degradation would produce straight lines. This relation applying in Arrhenius equation for first order reaction and get the straight line. The results plotted in figure 2 (a), (b), (c) and figure 3 (a), (b), (c) confirmed that the degradation of the polymer composites was indeed first order. The values of activation energy, frequency factors and error deviation were shown in Table 3 in 4(four) different temperatures 20 ^{0}C, 30 ^{0}C, 40 ^{0}C and 50 ^{0}C for SHMMA products of 49%, 59% and 71%. The values were found to be higher than that of the ungrafted one. These values increased with increase in the molecular weights i.e. increase in the grafting (%) in both of the degradation stages. The value of the correlation coefficients R was also calculated from the slope and intercept of the straight lines. It was noticeable that the change of the activation energy was significant in the grafted polymer composites. Contrarily, the decomposition temperature and activation energy of the grafted samples, which were produced at higher temperature, was increased (Table 4), suggesting that the high temperature provided favorable conditions to form more stable structures during the

grafting. The treatment also increased the crystallinity index of the fibers resulting in a higher degradation temperature

3.3 Differential Scanning Calorimetry

The thermal behaviour of ungrafted and SHMMA of different grafting (%) were studied with the help of DSC [34-35] at heating rate 20 ^{0}C/min and the thermograms are presented in figure 4. The thermal analysis data are given in Table 5(a). In case of ungrafted one, the first broad endotherm below 100 ^{0}C is due to the evaporation of water. Two minor and broad endothermic transition appeared at 234 ^{0}C and 297 ^{0}C (shoulder form), followed by a prominent endothermic peak at 370 ^{0}C.

In case of SHMMA, the endothermic peak due to the evaporation of water shifted to higher temperature as grafting increased. However, the SHMMA shown an endothermic peak at 107 ^{0}C (49% grafted), 120^{0}C (49% grafted) and 131 ^{0}C for 71% grafted product. The minor peaks (shoulder form) were shifted to 327, 335 and 347 ^{0}C for fibres due to enthalpic change and another endothermic peak was observed in each of grafted fibres at 390 ^{0}C (59% grafted), 400 ^{0}C (59% grafted) and 415 ^{0}C for 71% grafted fibre. Based on the above DSC results, it was assumed that the endothermic peaks at 435 ^{0}C, 450 ^{0}C, and 465 ^{0}C for the fibres were related to the presence of the MMA polymer in the silk fibre. The glass transition temperatures (Tg) for the grafted silk fibroin were shown in Table 5(a) 225, 260 and 275 for 49%, 59% and 71% SHMMA.

3.4 X-Ray Diffraction Studies

The XRD patterns of silk grafted with MMA are shown in figure 5 and the data obtained were tabulated in Table 5(b). The XRD patterns exhibited the presence of both amorphous and crystalline regions [36-37]. However, the crystalline regions were more prominent in case of grafted products, in comparison to original ungrafted silk fibre. From the data, it was evident that the crystalline (%) in SHMMA was found more than ungrafted one. The increase in crystalline character in SHMMA products indicated that on grafting, silk molecule had under gone an isomeric change, in other word, the silk molecule which was atactic had changed to isotactic after grafting with MMA using Ce^{IV} redox initiator system. Therefore, it might be suggested that the structural re-arrangement of SHMMA took place during grafting as given in Scheme 1. In this Scheme, the structure of Muga silk fibroin, which consisted mainly of amino acid residue of glycine, alanine, serine aspartic acid, tyrosine, and arginine has been represented in one dimension and the strategy was given to describe the way of attacking by the monomer free radical. The diagrammatic representation of SHMMA is given in Scheme 2.

3.5 Studies on Variation of Initiator and Acid Concentrations

The variation for concentrations of initiator - Ce^{IV} (cerric ammonium sulphate) was studied using five different concentrations from 15-35 x 10^{-3} M. It was evident from the Table 6 (a) that the rate of grafting (%) increased progressively with increasing the initiator concentration unto 30 x 10^{-3} M and decreased after that concentration. This might be expected at higher concentration of [Ce^{4+}] and is known to affect grafting by termination of growing grafted chains of SHMMA [38].

The variation of concentrations of H_2SO_4 was also studied from 13-21 x 10^{-2} M. The extent of grafting (%) increased progressively upto 19 x 10^{-2} M and there after tended to decrease shown in Table 6 (b). This was explained by the fact that ceric ion in water exists as Ce^{4+}, $[Ce(OH)_3]^{3+}$, and $[Ce–O–Ce]^{6+}$. With increase in sulphuric acid concentrations beyond 19 x 10^{-2} M, the equilibria shifted towards the formation of more and more Ce^{4+} and $[Ce(OH)_3]^{3+}$. Therefore, no further reactions take place and hence, the grafting (%) decreases.

IV. Conclusion

The thermosensitive biopolymer SHMMA was synthesized by graft copolymerization of methylmetacrylate (MMA) with cerric ammonium sulphate (Ce^{IV}) initiator onto biodegradable protein fibre *Anthearea assam* silk (SH). The influence of the content of MMA- Ce^{IV} grafted products have satisfactory results. From thermal studies it was observed that grafted SHMMA were found to be thermally more stable than that of the original one and the reaction follows the first order Arrhenius rate equation. The activation energy increases with the increase of the temperature ranges from 20-50 ^{0}C. Thus, the successful preparation of Silk fibroin with MMA monomer by graft co-polymerization techniques would provides a promising opportunity to widen potential application of silk fibroin in the biomaterials field.

Acknowledgment

The authors wish to thank the Acting Director, Dr. R. C. Baruah, North East Institute of Science & Technology (CSIR), Jorhat-785 006 for his kind permission to publish this paper.

References

1. Sing V, Tiwari A, Pandey S, Sing S K (2007). Peroxy-disulphat initiated synthesis of potato starch-graft PAN under microwave irradiation. Express Polymer letters. 1: 51-56.
2. Jin H J, Park J, Valluzzi R, Cebe P, Kaplan D L (2004). Structure and properties of silk hydrogels, Biomacromolecules. 5: 711–717.
3. Sashina E S, Bochek A M, Novoselov N P, Kirichenko D A (2006). Structure and solubility of natural silk fibroin. Russian J. Appl. Chem. 79: 869-876.
4. Hazarika L K, Saikia C N, Kataky A, Bordoloi S, Hazarika J (1998). Bioresource Tech. 64: 67-69.
5. Zhang K, Wang H, Huang C, Su Y, Mo X, Ikada Y (2009). Fabrication of silk fibroin blended P(LLA-CL) nanofibrous scaffolds for tissue engineering. J Biomed Mater Res. 43: 114-119 .
6. Enrico Marsanoa, Paola Corsinia, Maurizio Canettib, Giuliano Freddic (2008). Regenerated cellulose-silk fibroin blends fibers. International Journal of Biological Macromolecules. 43: 106-110.
7. Zhen-ding She, Wei-qiang Liu, Qing-ling Feng (2009). Preparation and cytocompatibility of silk fibroin/chitosan scaffolds. Frontiers of Materials Science in China. 3: 241-247.
8. Hoi-Yan Cheung, Kin-Tak Lau, Xiao-Ming Tao, David Hui (2008). A potential material for tissue engineering: Silkworm silk/PLA biocomposite. Composites Part B: Engineering. 39: 1026-1033.
9. Yin Tang, Chuanbao Cao, Xilan Ma, Chen Chen, Hesun Zhu (2006). Study on the preparation of collagen-modified silk fibroin films and their properties. Biomed. Mater. 1: 242-246.
10. Hyoung-Joon Jin, Jaehyung Park, Regina Valluzzi, Peggy Cebe, Kaplan David L (2004). Biomaterial Films of *Bombyx Mori* Silk

Fibroin with Poly(ethylene oxide). Biomacromolecules. *5* (3): 711–717.

11. Kim D-H (2009). Silicon electronics on silk as a path to bioresorbable, implantable devices. Appl. Phys. Lett. 95: 133701-133703.
12. Amsden J J (2009). Spectral analysis of induced colour change on periodically nanopatterned silk films. Opt Express. 17: 21271-21279.
13. Parker S T (2009). Biocompatible silk printed optical waveguides. Adv. Mater. 21: 2411-2415.
14. Ali H, Ebrahim V-F (2008). Kinetic study of methacrylate copolymerization systems by thermoanalysis methods. J Appl Sci. 109: 3302-3308.
15. Brandrup J, Immergut E H, Grulke E A, editors. Polymer Hand Book, 4th Edn., Wiley : New York, 1999.
16. Kessler M R, White S R (2002). Cure kinetics of the ring-opening metathesis polymerization of dicyclopentadiene. J Polym Sci Part A : Polym Chem. 40: 2373.
17. Choudhury S N. Editor. Silk and Sericulture, first ed. Directorate of Sericulture; Assam: India, 1992.
18. Liu Y, Yang L, Shi Z, Li J (2004). Graft copolymerization of methyl acrylate onto cellulose initiated by potassium ditelluratoargentate (III). Polymer International. 53: 1561-1566.
19. Singha A S, Shama A, Thakur V K (2008). Pressure induced graft-co-polymerization of acrylonitrile onto Saccharum cilliare fibre and evaluation of some properties of grafted fibre. Bull. Mater. Sci. 31: 7-13.
20. Flynn J H, editor. In Encyclopedia of Polymer Science and Engineering, wiley, New York, 1989,
21. Wang J, Wenhui Wu, Zhihui Lin (2008). Kinetics and thermodynamics of the water sorption of 2-hydroxyethyl methacrylate/styrene copolymer hydogels. J Appl Polym Sci. 109(5): 3018-3025.
22. Budrugeac P, Segal E (2003). On the nonlinear isoconversional procedures to evaluate the activation energy of nonisothermal reactions in solids. J Chem Kinetics. 36: 87-92.
23. Coats A W, Redfern J R (1964). Kinetic Parameters from Thermogravimetric Data. Nature. 68: 201-211.
24. Kaushik R K, Gur I S, Bhatnagar H L (1989). Thermal degradation of cellulose, cellulose thiophosphate and its complexes with transition-metal cations. Thermochim. Acta. 145: 331–352.
25. Broido A (1969). A simple, sensitive graphical method of treating thermogravimetric analysis data. J Polym Sci. 7:1761–1773.
26. Rabek J F. editor. Experimental methods in polymer chemistry, John Wiley & Sons: London, 1980.
27. Jian M J, Hui J Z, Guang L, Jin J H, Sheng L Y (2008). Poly (P-phenylene benzoxazole) fibre chemically modified by the incorporation of sulfonate groups. J Appl Polym Sci. 109: 3133-3137.
28. Kaith B S, Kalia S (2008). Graft copolymerization of MMA onto flax under different reaction conditions : a comparative study. Express Polymer letters. 2: 93-101.
29. Bhattacharyya A, Misra B N (2004). Grafting : A versatile mean to modify Polymers techniques, factors and applications. Progress in Polymer Science. 29: 767-773.
30. Margutti S, Cicini S, Projetti N, Capitani D, Conio G, Pedemonte E, Segre A L (2002). Physical-chemical characterization of acrylic polymers grafted on cellulose. Polymer. 43: 6183-6189.
31. Mingzhong Li, Norihiko Minoura, Lixing Dai, Linsen Zhang (2001). Preparation of Porous Poly(vinyl alcohol)-Silk Fibroin (PVA/SF) Blend. Membranes. 286: 529 – 533.
32. Rahman M R, Huque M M, Islam M N, Hasan M (2008). Improvement of physico-mechanical properties of jute fiber reinforced polypropylene composites by post-treatment. Comp Pt A. 39:1739–1747.
33. Isil A, Gulin S P, Saadet O (2008). Thermal oxidative degradation kinetics and thermal properties of poly(ethylene terephthalate) modified with poly(lactic acid). J Appl Polym Sci. 109: 2747-2751.
34. Jingxin Zhu, Huili Shao, Xuechao Hu (2007). Morphology and structure of electrospun mats from regenerated silk fibroin aqueous solutions with adjusting pH. International Journal of Biological Macromolecules. 41: 469-474.
35. Cheung Hoi-Yan, Lau Kin-Tak, Tao Xiao-Ming, Hui David (2008). A potential material for tissue engineering: Silkworm silk/PLA biocomposite. Composites Part B: Engineering. 39: 1026-1033.
36. Spinger V. editor. Worked Examples in X-ray Analysis (Supplied with the Computer Controlled XRD; Type JDX-11P 3A, JEOL, Japan, Spinger: Berlin, 2006.
37. Singha A S, Kaith B S, Chauhan A, Misra B N (2006). Mechanical properties of natural fibre reinforced polymer composites. J Polym Mater. 23: 3456-3460.
38. Das A M, Chowdhury P K, Saikia C N, Rao P G (2009). Some Physical properties and structure determination of Vinyl monomer-grafted Anthearea assama silk fibre. 48: 9338-9345.

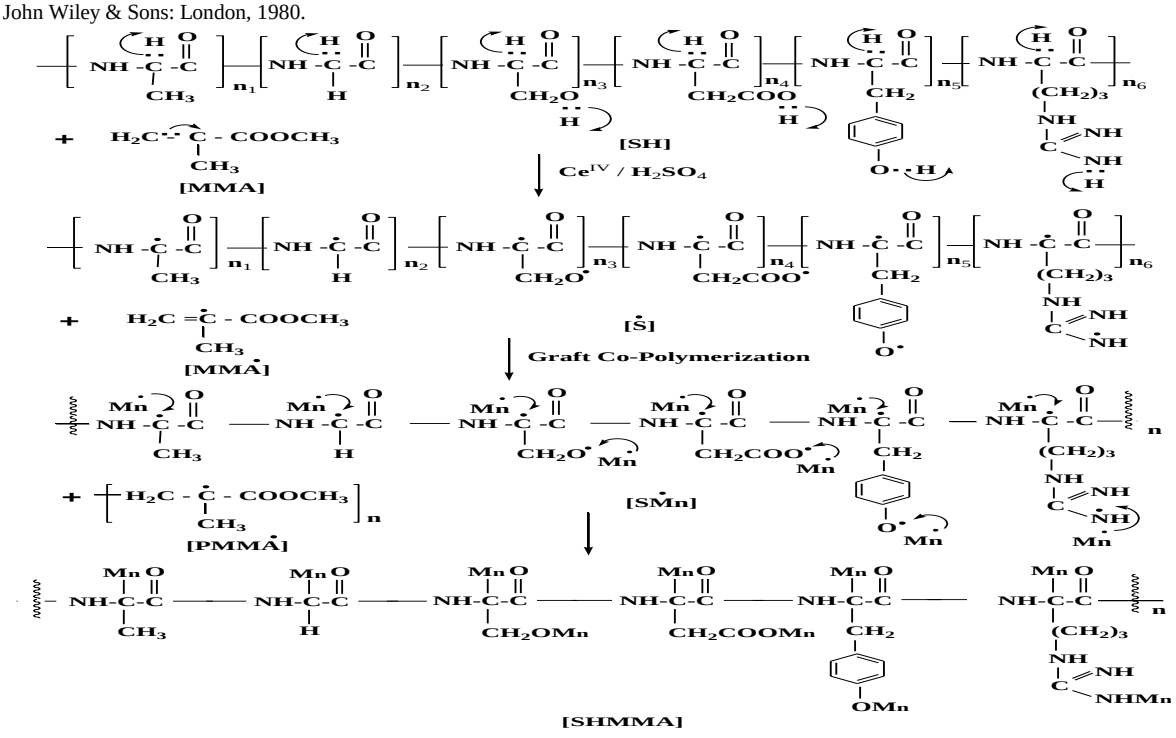

Where, SH- silk molecule, S·-silk free radical, Mn represent the polymethylmethacrylate (PMMA).

Scheme 1 : Schematic representation of the structural changes during graft copolymerization of the SH.

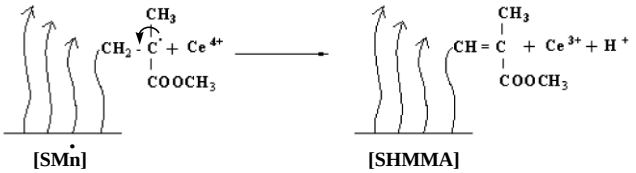

Scheme 2 – Diagrammatic representation of grafted silk molecule.

List of Table, Figures have been given below.

Table 1 - (a) Thermal analysis data : Active decomposition temperature and weight loss for ungrafted and SHMMA at heating rates 20 ^{0}C/min
(b) DTA - decomposition temperature.

Table 2 - (a) Thermal analysis data : Active decomposition temperature and weight loss for ungrafted and SHMMA at heating rates 30 ^{0}C/min
(b) DTA – decomposition temperature.

Table 3 - The Experimental Conditions and Kinetic data of Broido Equation.

Table 4 - Logarithmic data using Arrhenius Equation at different stages (From Broido Equation).

Table 5 - (a) Thermal analysis data for decomposition temperature and glass transition (Tg) values of ungrafted and SHMMA at heating rate at 20^{0}C/min.
(b) X-ray diffraction data and crystallinity of ungrafted and SHMMA.

Table 6 - Grafting on *Antheraea assama* silk composites by MMA-Ce^{IV} system
(a) Variation of Ce^{IV} initiator
(b) Variation of H_2SO_4 acid

Figure 1 : Thermo-gravimetric analysis (TGA), Differential thermo-gravimetry (DTG) and Differential thermal analysis (DTA) curves at heating rate 20 ^{0}C/min – (a) ungrafted, (b) 49% SHMMA, (c) 59% SHMMA and (d) 71% SHMMA

Figure 2 : Plots of ln *k* vs 1/T of the second stage thermal decomposition of SHMMA using Arrhenius Equation data from Broido Equation – (a) 49%, (b) 59% and (c) 71%.

Figure 3 : Plots of ln *k* vs 1/T of the second stage thermal decomposition of SHMMA using Arrhenius Equation data from Broido Equation – (a) 49%, (b) 59% and (c) 71%.

Figure 4 : Differential scanning calorimetry (DSC) curves for the decomposition of – (a) ungrafted, (b) 49%, (c) 59% and (d) 71% SHMMA.

Figure 5 : XRD patterns of the (a) ungrafted, (b) 49%, (c) 59% and (d) 71% SHMMA.

Table 1 - (a) Thermal analysis data : Active decomposition temperature and weight loss for ungrafted and SHMMA at heating rates 20 ^{0}C/min
(b) DTA - decomposition temperature.

(a)		Weight loss, %			Active decomposition temperature			(b) DTA Data		
Samples	%	20 ^{0}C/min			20 ^{0}C/min			20 ^{0}C/min		
--	--	I	II	III	I	II	III	I	II	--
Ungrafted	--	12.5 (30-140)	41.8 (150-390)	43.0 (390-640)	60 (endo)	360 (endo)	520 (endo)	150 (endo)	350 (endo)	---
Grafted	49	10.2 (30-170)	38.0 (175-430)	45.5 (440-675)	80 (endo)	380 (endo)	550 (endo)	175 (endo)	395 (endo)	365 (exo)
	59	8.9 (30-180)	36.8 (185-450)	48.8 (455-695)	90 (endo)	390 (endo)	565 (endo)	182 (endo)	420 (endo)	380 (exo)
	71	7.2 (30-190)	33.0 (195-470)	47.5 (480-720)	95 (endo)	400 (endo)	585 (endo)	200 (endo)	435 (endo)	405 (exoo)

I, II, II-pre, second and third stages. Temperature range (in ^{0}C) in parentheses.

Table 2 - (a) Thermal analysis data : Active decomposition temperature and weight loss for ungrafted and SHMMA at heating rates 30 ^{0}C/min
(b) DTA – decomposition temperature.

(a)		Weight loss, %			Active decomposition temperature			(b) DTA Data		
Samples	%	30 ^{0}C/min			30 ^{0}C/min			30 ^{0}C/min		
--	--	I	II	III	I	II	III	I	II	--
Ungrafted	--	13.8 (30-160)	48.0 (170-400)	32.0 (400-700)	70 (endo)	365 (endo)	540 (endo)	160 (endo)	355 (endo)	---
Grafted	49	11.8 (30-175)	46.5 (180-420)	35.8 (430-720)	80 (endo)	385 (endo)	570 (endo)	190 (endo)	415 (endo)	380 (exo)
	59	9.6 (30-190)	43.9 (195-440)	39.7 (445-740)	90 (endo)	390 (endo)	585 (endo)	200 (endo)	430 (endo)	405 (exo)
	71	8.5 (30-195)	41.8 (205-455)	37.0 (460-760)	95 (endo)	410 (endo)	605 (endo)	210 (endo)	455 (endo)	420 (exoo)

I, II, III-pre, second and third stages. Temperature range (in ^{0}C) in parentheses.

Table 3 - The Experimental Conditions and Kinetic data of Broido Equation.

Samples	Temperature	I (First Stage)			II (Second Stage)		
%-Grafted	^{0}C	E KJ mol^{-1}	A S^{-1}	SED S^{-1}	E KJ mol^{-1}	A S^{-1}	SED S^{-1}
49	20	34.421	0.428	0.003	39.552	0.579	0.001
	30	37.830	0.539	0.005	43.415	0.810	0.001
	40	41.011	0.659	0.001	55.859	1.268	0.004
	50	45.314	0.824	0.002	58.057	1.752	0.007
59	20	39.104	0.572	0.002	48.011	0.915	0.003
	30	42.755	0.880	0.004	54.372	1.328	0.001
	40	45.004	1.284	0.001	62.430	1.802	0.002
	50	48.910	1.817	0.003	67.576	2.416	0.002
71	20	45.092	0.931	0.005	56.710	1.394	0.004
	30	56.380	1.296	0.002	66.476	1.870	0.006
	40	59.314	1.820	0.004	69.942	2.411	0.001
	50	62.568	2.541	0.001	77.642	2.914	0.003

Table 4 - Logarithmic data using Arrhenius Equation at different stages (From Broido Equation).

Samples	Temperature	I (First Stage)			II (Second Stage)		
%-Grafted	Kelvin	1/T	ln *k*	R^2	1/T	ln *k*	R2
49	293	0.0034	-0.863	0.9993	293	-0.562	0.9962
	303	0.0033	-0.633	--	303	-0.228	--
	313	0.0032	-0.433	--	313	0.216	--
	323	0.0031	-0.211	--	323	0.539	--
59	293	0.0034	-0.573	0.9977	293	-0.109	0.9966
	303	0.0033	-0.145	--	303	0.262	--
	313	0.0032	0.233	--	313	0.565	--
	323	0.0031	0.579	--	323	0.857	--
71	293	0.0034	-0.09	1	293	0.309	0.9911
	303	0.0033	0.237	--	303	0.60	--
	313	0.0032	0.58	--	313	0.853	--
	323	0.0031	0.91	--	323	1.041	--

Table 5 - (a) Thermal analysis data for decomposition temperature and glass transition (Tg) values of ungrafted and SHMMA at heating rate at 20^0C/min.
(b) X-ray diffraction data and crystallinity of ungrafted and SHMMA.

(a)				(b)		
Samples	%	Decomposition Temperature (°C)	Tg (°C)	X-ray diffraction data(d' spacing in A°)	2θ	Crystsll -inity (%)
Ungrafted	--	92	175	6.772 (100)*	9.03	33
	--	234	175	**4.553 (72)**	18.40	33
	--	297	175	**3.825 (65)**	20.02	33
	--	370	175	--	--	--
Grafted	49	107	225	7.927 (100)	12.05	46
	49	327	225	**5.726 (87)**	18.36	46
	49	390	225	**4.821(81)**	22.51	46
	49	435	225	--	--	--
	59	120	260	**8.234 (100)**	13.54	54
	59	335	260	**7.231 (89)**	19.32	54
	59	400	260	**5.822 (83)**	22.65	54
	59	450	260	--	--	--
	71	131	275	10.021 (100)	13.78	62
	71	347	275	**8.019 (93)**	22.98	62
	71	415	275	6.246 (77)	27.32	62
	71	465	275	--	--	--

Table 6 - Grafting on Antheraea assama silk composites by MMA-Ce^{IV} system
(a) Variation of Ce^{IV} initiator
(b) Variation of H_2SO_4 acid

		(a)					(b)				
Grafting Parameters	Time of Reaction, h	Ce^{IV} initiator Concentration M (Mol/L)					H_2SO_4 acid Concentration M (Mol/L)				
		15	20	25	30	35	13	15	17	19	21
Graft Yield (%)	1	33	39	47	58	51	28	31	40	49	44
	2	37	45	54	63	56	33	39	47	58	51
	3	43	50	61	68	65	36	44	51	62	54
	4	50	58	69	76	72	41	52	59	71	63
	5	45	53	64	71	67	38	46	54	65	58
Total Conversion (%)	1	12.4	15.1	17.8	20.1	17.9	11.3	13.4	15.9	17.5	15.6
	2	15.2	18.3	23.0	24.8	23.7	12.4	15.1	17.8	20.1	17.9
	3	17.5	20.0	25.2	28.3	26.2	14.9	18.3	21.3	24.5	22.2
	4	19.0	23.1	28.0	32.0	29.0	16.7	18.9	22.8	28.0	25.3
	5	18.0	21.0	26.0	29.0	26.9	15.6	17.7	22.0	25.2	23.0
Grafting Efficiency (%)	1	37.9	38.8	39.3	42.6	41.8	35.5	37.2	37.9	40.8	38.3
	2	39.0	40.9	41.0	44.0	42.4	37.9	38.8	39.3	42.6	41.8
	3	40.8	42.0	43.0	45.0	43.8	38.2	39.4	40.7	42.9	42.0
	4	42.0	43.3	44.5	46.7	45.0	40.2	41.0	42.0	43.5	42.6
	5	41.2	42.7	43.6	45.5	44.2	39.0	40.1	41.6	43.1	42.3
Rate of Grafting x 10^6	1	6.1	3.6	2.9	2.7	1.9	5.2	2.9	2.5	2.3	1.6
	2	6.8	4.2	3.3	2.9	2.1	6.1	3.6	2.9	2.7	1.9
	3	8.0	4.6	3.8	3.1	2.4	6.7	4.1	3.1	2.9	2.0
	4	9.3	5.4	4.3	3.5	2.7	7.6	4.8	3.6	3.3	2.3
	5	8.4	4.9	3.9	3.3	2.5	7.0	4.3	3.3	3.0	2.1

The results are averages of three readings.
Silk composites 1 g, MMA 50 x 10^{-2} M, Temperature 50 ^{0}C and material to liquor ratio 1:150 (M = molar), **(a)** H_2SO_4 acid 15 x10^{-2} M, **(b)** Ceric ammonium sulphate 15 x10^{-3} M.

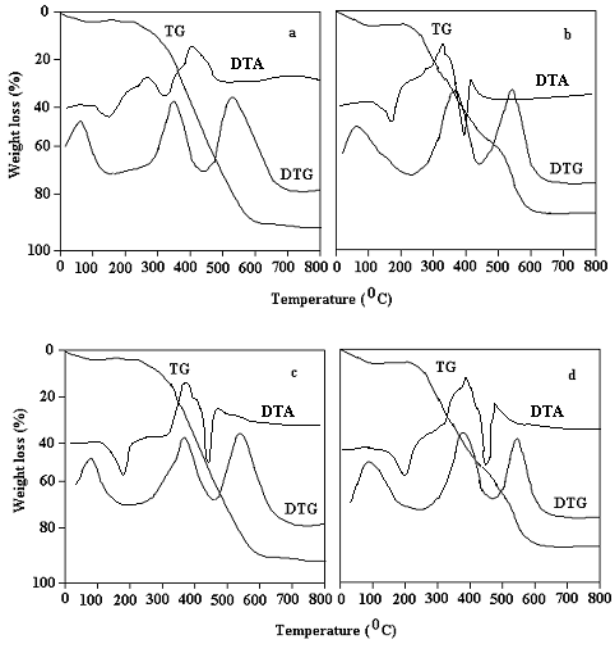

Figure 1 : Thermo-gravimetric analysis (TGA), Differential thermo-gravimetry (DTG) and Differential thermal analysis (DTA) curves at heating rate 20 ^{0}C/min – (a) ungrafted, (b) 49% SHMMA, (c) 59% SHMMA and (d) 71% SHMMA

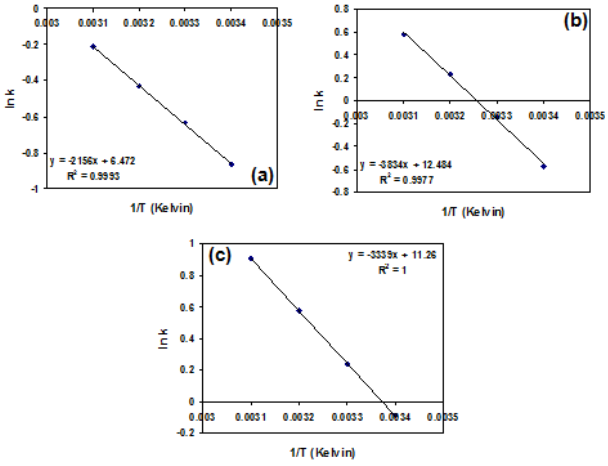

Figure 2 : Plots of ln *k* vs 1/T of the second stage thermal decomposition of SHMMA using Arrhenius Equation data from Broido Equation – (a) 49%, (b) 59% and (c) 71%.

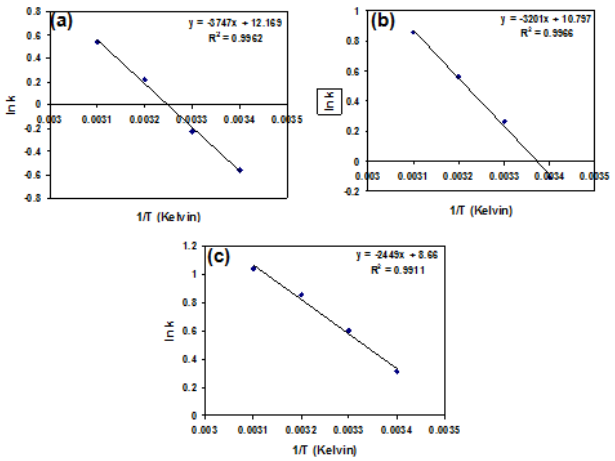

Figure 3 : Plots of ln *k* vs 1/T of the second stage thermal decomposition of SHMMA using Arrhenius Equation data from Broido Equation – (a) 49%, (b) 59% and (c) 71%.

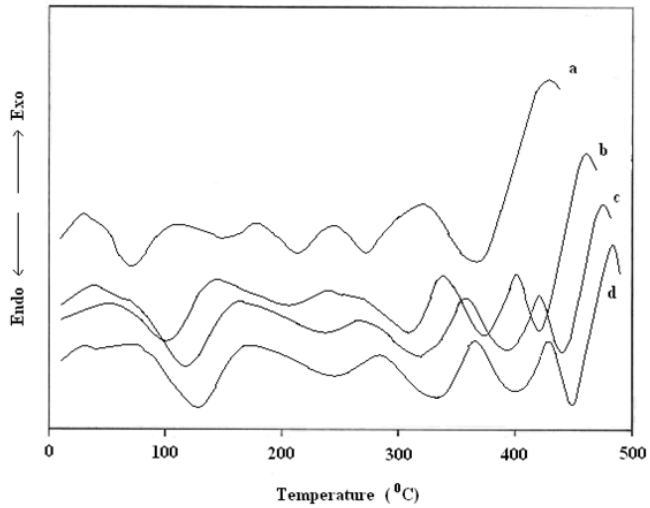

Figure 4 : Differential scanning calorimetry (DSC) curves for the decomposition of – (a) ungrafted, (b) 49%, (c) 59% and (d) 71% SHMMA.

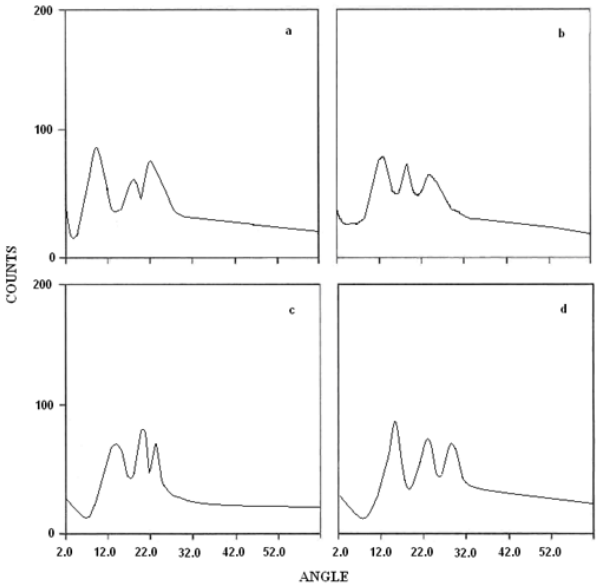

Figure 5 : XRD patterns of the (a) ungrafted, (b) 49%, (c) 59% and (d) 71% SHMMA.